Sensors & Transducers, Vol. 162 , Issue 1, January 2014, pp. 29-37

www.sensorsportal.com

Sensors & Transducers

http://www.sensorsportal.com

Optimal Design of Electromagnetic Acoustic Transducer Used to Generate Lamb Wave

[1] Yan LIU, [2] Yuemin WANG, [2] Longxiang ZHU, [2] Fengrui SUN

[1] College of Arts and Science, Naval University of Engineering,
Hubei Wuhan, 430033, China
[2] College of Ship & Power, Naval University of Engineering,
Hubei Wuhan, 430033, China
[1] E-mail: greerliu@126.com

Received: 12 November 2013 /Accepted: 9 January 2014 /Published: 31 January 2014

Abstract: Electromagnetic ultrasonic transducer is the core component of the electromagnetic ultrasonic testing equipment. This paper establishes a three-dimensional model of the electromagnetic ultrasonic transducer used to generate Lamb wave, then by uniform design experiment and finite element analysis, the paper obtains the law between the eddy current density, the conductor width, length of the coil, the lift off distance, and the permanent magnets thickness. The law is verified by the experiment. It provides an overall principle for the optimal design of electromagnetic ultrasonic transducer. *Copyright © 2014 IFSA Publishing, S. L.*

Keywords: EMAT, Lamb wave, Finite element analysis, Optimal design.

1. Introduction

Electromagnetic ultrasonic transducer is a non-contact ultrasonic transmitter and receiver apparatus. The transducer mechanism includes Lorentz force, magnetostrictive force and magnetic force. The main advantage of an EMAT over a conventional Piezoelectric ultrasonic transducer is that no couplant is needed; thus, measurement inconsistency arising from couplant use during the non-destructive inspection can be eliminated. Now, EMAT is widely used [1-3] in defect detection of the base metal, detection of the weld, thickness measurement, detection of the composite material, detection of railway tracks and wheels, stress measurement and high temperature detection. Compared with the traditional Piezoelectric ultrasonic transducer, the main deficiency of an EMAT is its relatively low conversion efficiency, therefore, the design of an EMAT is essential. B. Dutton [4] describes a new EMAT design using a finite element software, and the magnetic flux density was increased from 0.29 T to 0.52 T. Koorosh Mirkhani [5] developed a complete modeling system for an EMAT, gave the complete and detailed calculation of the static magnetic flux, and provided the design basis for the rational allocation of the magnetic field. Shujuan Wang [6] provided a 3-D finite element analysis for EMAT used in the detection for the aluminum surface and near-surface; and as the goal to improve the efficiency of the EMAT, the geometric parameters of the transducer had been optimized. Hongxiu Zhu [7] established the relationship between the function of the magnetic flux density and molecular vibration amplitude, and used the uniformity experiment to optimize EMAT. These studies focused on the depth exploration of the EMAT work mechanism, and the cognitive of the transmitting and receiving physical processes,

involved in the overall design standards of the EMAT, and the overall aim to optimize the design.

In this paper, the finite element software is applied to EMAT three-dimensional finite element analysis for steel surface detection, and the geometric parameters of transducer are optimized to the overall design and configuration of the permanent magnet, coil, and lift-off distance. So that there is no need in signal post-processing to improve the signal-to-noise ratio and the conversion efficiency of the EMAT. The work reported here is divided into four parts. First, electromagnetic field equation is developed to calculate the Lorentz force distribution. Second, a 3D finite element model is used to optimize the design of the EMAT system. Third, by uniform design experiment and finite element analysis, the paper obtains the law between the eddy and the conductor width, length, the lift off distance, and the permanent magnets thickness. Finally, the effectiveness of the optimized design results is verified by the detection of steel plate.

2. Analytical Study of Lamb Wave Characteristics

Lamb wave can be generated in a plate with free boundaries with an infinite number of modes for both symmetric and antisymmetric displacements within the layer. The symmetric modes are also called longitudinal modes because the average displacement over the thickness of the plate or layer is in the longitudinal direction. The antisymmetric modes are observed to exhibit average displacement in the transverse direction and these modes are also called flexural modes. Lamb wave frequency characteristic with free boundary conditions is:

Symmetric modes:

$$\frac{\tan k_{0s}d}{\tan k_{0l}d} = -\frac{4k_0^{\ 2}k_{0l}k_{0s}}{(k_0^{\ 2}-k_{0s}^{\ 2})^2}, \tag{1}$$

Antisymmetric modes:

$$\frac{\tan k_{0s}d}{\tan k_{0l}d} = -\frac{(k_0^{\ 2}-k_{0s}^{\ 2})^2}{4k_0^{\ 2}k_{0l}k_{0s}}, \tag{2}$$

where

$$k_{0l}^2 = \left[\frac{\omega}{c_l}\right]^2 - k_0^2, \tag{3}$$

$$k_{0s}^2 = \left[\frac{\omega}{c_s}\right]^2 - k_0^2, \tag{4}$$

where c_S - transverse wave speed, c_L - longitudinal wave speed.

Although the equations look simple, they can be solved only by numerical methods. To an example of symmetric modes, the formulation (3) and formulation (4) are substituted into the formulation (1) results in:

$$\frac{\tan\dfrac{2\pi\sqrt{c_p^2-c_s^2}\,fd}{c_p c_s}}{\tan\dfrac{\sqrt{c_p^2-c_l^2}}{c_p c_l}} = -\frac{4c_s^3\sqrt{(c_p^2-c_l^2)(c_p^2-c_s^2)}}{c_l(2c_s^2-c_p^2)^2}, \tag{5}$$

where phase velocity $c_p = \omega/k$.

Phase velocity of each mode and frequency-thickness *fd* are non-linear relationship.

The group velocity c_g can be found from the phase velocity c_p by use of the formula:

$$c_g = c_p^2\left[c_p - (fd)\frac{dc_p}{d(fd)}\right]^{-1}, \tag{6}$$

The numerical solution of the results [8] is showed in Fig. 1.

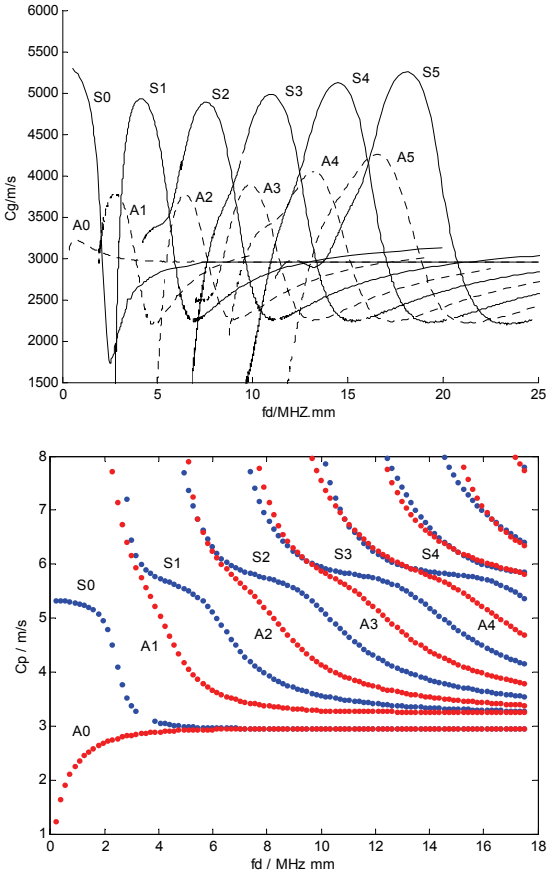

Fig. 1. Dispersion curves for a traction-free steel plate.

3. Use EMAT to Generate Lamb Wave

The core of the EMAT technology is electromagnetic ultrasonic transducer, the essential difference between the EMAT and a conventional piezoelectric ultrasonic transducer is transmitting and receiving mode, EMAT transmits and receives ultrasonic waves by electromagnetic effect. Its energy is converted directly in the skin layer of the workpiece surface, so it is no need to contact with the workpiece and any coupling medium. The probe structure of the EMAT used to generate Lamb wave in the ferromagnetic material was shown in Fig. 2. The two primary components of an EMAT [9] are a mender coil that is fed by a very large alternating current pulse, and a magnet designed to produce a strong static magnetic flux within the skin depth of the test specimen directly below the EMAT coil.

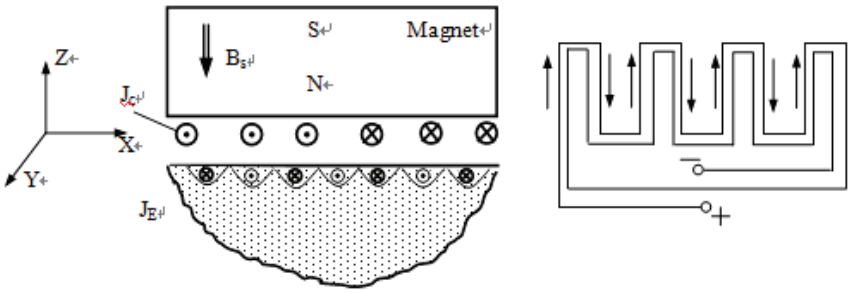

Fig. 2 The mechanism for Lamb wave generation by magnetostrictive type EMATs.

As can be seen from Fig. 2, the pulsed alternating current $J_C = Ie^{iwt}$ fed to the transmitter EMAT coil induces dynamic magnetic field B_d within the skin depth of the test piece. If the displacement current is ignored, according to Ampere's law, it induces eddy currents J_E. In the presence of a large bias magnetic flux B_S; theses eddy currents lead to generate body forces f_L on the surface layer of the specimen. These forces lead to generate an ultrasonic wave into the specimen. According to the principles of electromagnetism [6]. The above process can be expressed as:

$$\nabla \times H_{d,m} = J_C, \tag{7}$$

$$B_{d,m} = \mu_m H_{d,m}, \tag{8}$$

$$\nabla \times E_E = -\frac{\partial B_{d,m}}{\partial t}, \tag{9}$$

$$J_E = \gamma E_E, \tag{10}$$

$$f_L = J_E \times (B_{d,m} + B_S), \tag{11}$$

where $H_{d,m}$ is the strength of the magnetic field generated by the emission current; J_C is the emission current density; $B_{d,m}$ is the magnetic flux density generated by the emission current in the plate; μ_m is the relative magnetic permeability of the steel; J_E is the eddy current density; B_S is the static magnetic field generated by the EMAT magnets; f_L is the radiesthesia. The theoretical model is established to solve the simultaneous dynamic equations of electromagnetic field elastic stress and strain; get the stress in the material lattice, then it is imported to sports displacement equation and gets the displacement of the ultrasonic wave field [10]. EMAT is not simply the combination of eddy current coil and the fixed external magnetic field, the metal surface is an important part of the transducer, electro-acoustic conversion relies on the metal surface. When the body wave wavelength is much larger than the skin depth, and the loss caused by the diffraction and the noise generated by the amplifier are ignored, the signal-to-noise ratio can be expressed as [11]:

$$V_{EMAT}/V_{noise} = (p_0)^{\frac{1}{2}} B^2 A \exp(-aG/D)/[W^2 Z_{LS}(4KT\beta)^{\frac{1}{2}} R_0], \tag{12}$$

where p_0 is the input power of the transmitter coil; R_0 is the coil resistance per unit area; W is the width of the coil. As can be seen from the formula, the most critical factor which affects the efficiency of the system is the bias magnetic induction strength. It is proportional to the Lorentz force and magnetostriction force. To raise the strength of the external magnetic field can increase the particle velocity and sound intensity, and improve the signal-to-noise ratio and detection sensitivity. Thus, the design principles of the EMAT magnet is formed a strong deflection magnetic field in the medium surface and near surface.

4. Optimal Design of the EMAT

4.1. EMAT finite Element Modeling

Finite element analysis based on the variational principle solves a class of partial differential equations from a new perspective, not only the solve performance is good, but also the solve accuracy is higher. It is an effective numerical methods used in EMAT model. (7)-(11) is a typical problem of eddy current field, can be solved with the finite element theory. According to the structure and operating characteristics of the electromagnetic ultrasonic nondestructive testing device, a 3-D EMAT solid model includes [6, 12]: Nd-Fe-B permanent magnet, EMAT coil, the test specimen, and air field.

The advantage of using a permanent magnet is that the magnet size is small, and the entire design of the EMAT transducer can become compact. Generally, the forms of the permanent magnet are cylindrical and horseshoe-shaped, permanent magnet group can also be used to provide the deflection magnetic field. This paper focuses on the cylindrical permanent magnet, as shown in Fig. 3. The size of Nd-Fe-B permanent magnet is $25\ mm \times 25\ mm \times 12.5\ mm$, the type is N35, the remanence is 1.21 T, the coercive force is 915 KA/m, and the maximum magnetic energy product is 279 J/m^3.

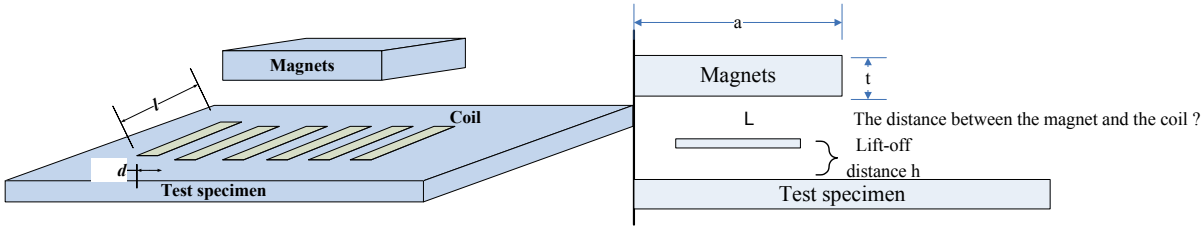

Fig. 3. The EMAT 3D solid model.

The design principle of EMAT coil is to improve the conversion efficiency of the coil. The coil spacing must be designed to meet the phase matching conditions, that is, coil spacing is equal to half of the Lamb wavelength.

$$d = \frac{\lambda}{2} = \frac{c_p}{2f}, \tag{13}$$

where λ is the wavelength, C_P is the wave velocity, f is the frequency, d is the center distance of two adjacent conductors. In this paper, the excitation coil uses a mender coil, and the coil resistivity is $1.68 \times 10^{-8} \Omega \cdot m$. Because the length of the coil is much larger than the spacing, the meander coil can be simplified as unconnected and parallel wires. The size of the wires is $30\ mm \times 0.5\ mm \times 0.5\ mm$, the number is 8, and the lift off distance is 0.1 mm. The hollow cylindrical coil can be regarded as stranded coil unit. The finite element model uses solid97 carrier unit.

The relative magnetic permeability of the test specimen is 500, the resistivity is $9.18 \times 10^{-8} \Omega \cdot m$, the relative magnetic permeability of the air and the coil is 1. The size of air field should be 3-5 times the EMAT model size, its size is selected as $900\ mm \times 900\ mm \times 500\ mm$. Taking into account the skin effect of the eddy current in the metal surface of the test piece, the unit split is refined. The finite element model of the test specimen uses Solid45, a 3-D electromagnetic structure coupling unit. U_x , U_y , and U_Z are displacement degrees of freedom, electromagnetic analysis result as a load is applied to the test specimen to analyze the internal particle stress, strain and displacement. Taking into account the skin effect, the specimen surface has done mesh refinement [5], as shown in Fig. 4.

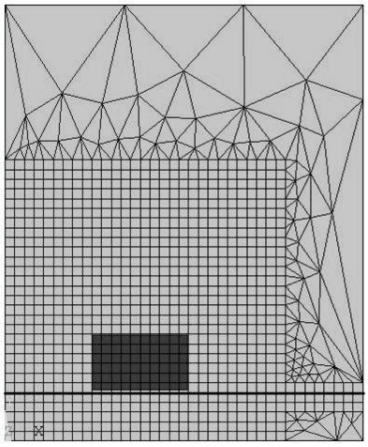

Fig. 4. FEM mesh.

According to the electromagnetic ultrasonic excitation mechanism, excitation is applied to coil using time-varying current [13], that sinusoidal signal with peak current 100 A and operating frequency 500 kHz, signal waveform is shown in Fig. 5.

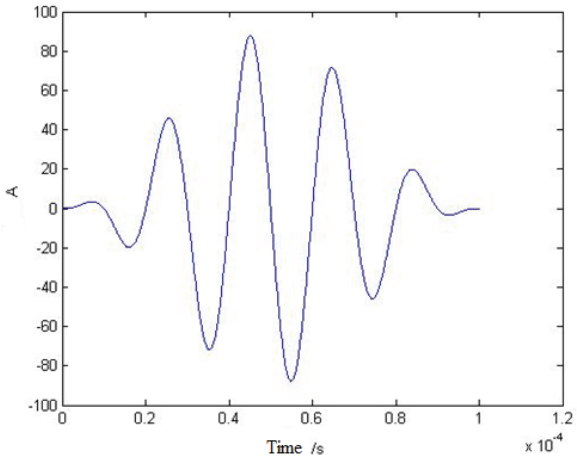

Fig. 5. Signal waveform diagram.

Surface wave velocity in the test specimen is $v = 2310\ m/s$, calculated by $f \cdot \lambda = v$, the surface wavelength is about 4.6 mm. Coil spacing and λ should meet with phase-matching condition, so the coil spacing is about 2.3 mm.

The analysis is processed using general postprocessor POST1 and time history postprocessor POST26 [14]. The result was picked up to do electromagnetic structure coupling when the excitation current reaches the first peak. Fig. 6 shows the magnetic flux density profile from a single cylindrical permanent magnet, with the magnet orientation shown below in profile.

As can be seen from the figure, magnetic induction in the center position is strong and weak at the edge, within the scope of the coil area, the B_S value distribution of the test specimen surface is stabilized, and has small fluctuations. The maximum flux density reaches to 2.43 T, which coincide with the theoretical analysis.

Therefore, in order to excite strong magnetic induction force and electromagnetic ultrasonic with limited volume of the probe, the static magnetic field should be concentrated in the vortex flow region, and reasonable distribution of the eddy current field and the static magnetic field is essential for improving the EMAT transducer efficiency.

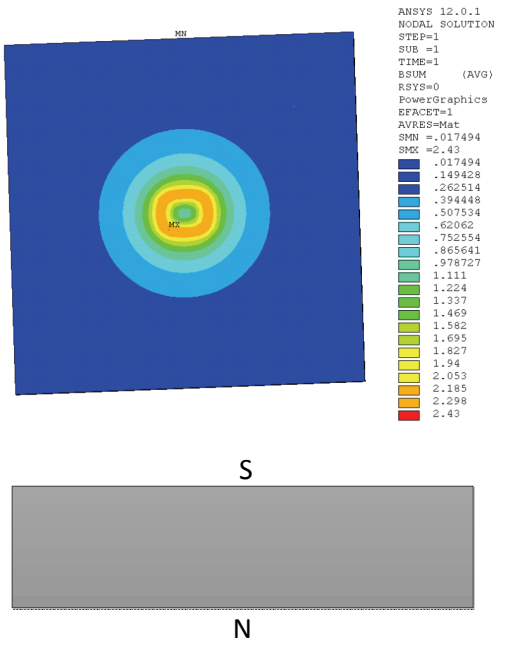

Fig. 6. Measured magnetic flux density profile of a cylindrical EMAT.

4.2. The Optimal Design of EMAT Coil

The EMAT transducer efficiency is extremely sensitive to the variation of the parameters of the excitation coil, and the change of the lift-off distance between the excitation coil and the test specimen. According to the eddy current distribution pattern in the test specimen, the maximum eddy current density J is as a research object to the study the relationship between the three factors of the excitation coil length l, width d and lift-off h and the eddy current density. Fig. 2 is the EMAT 3-D solid model [12]. The ranges of the three factors are: l : 30-50 mm; d : 0.5-1.5 mm; h : 0.1-1.0 mm. A small number of experiments are needed to find the analytical conditions with uniform experimental design, in this paper, uniform experimental design is used [7]. Uniform design uses a table to arrange experiment, and uniform table is constructed based on the application principle of multi-dimensional numerical integration. Each table has a uniform design code $U_n(n^m)$, where U represents uniform design, The subscript n denotes the number of

experiments, m denotes that the table has m column. Three design variables of the excitation coil length l, width d and lift-off h are divided into 10 equal portions, and there are 11 experiments. The maximum eddy current density J is calculated by ANSYS finite element software, are listed in Table 1.

Table 1. Uniform test of 3 elements for EMAT coil $U_{11}(11^3)$.

No.	The length of coil $l(mm)$	The width of coil $d(mm)$	Lift-off distance $h(mm)$	Eddy current density $J(10^6 A/m^2)$
1	30	0.9	0.7	218
2	32	1.4	0.3	298
3	34	0.8	1.0	183
4	36	1.3	0.6	308
5	38	0.7	0.2	251
6	40	1.2	0.9	251
7	42	0.6	0.5	223
8	44	1.1	0.1	262
9	46	0.5	0.8	212
10	48	1.0	0.4	274
11	50	1.5	1.1	240

As can be seen from the Table 1, the eddy current density of the test specimen changes with the influence of the excitation coil length, width, and liftoff distance. Therefore, the optimal combination of the coil parameters is: the length is 36 mm, the width is 1.3mm, and the lift-off distance is 0.6 mm.

4.3. The Optimal Design of EMAT Permanent Magnet

There are two principle [15] of EMAT magnet design, the first one is to be able to produce high-intensity magnetic field, the second one is to make the design structure compact. In order to form strong deflection magnetic field in the medium surface and near surface, it is needed to use the high-strength magnet. Permanent magnets and electromagnets can be used. The advantage of using permanent magnet is the size of the magnet is small, so the EMAT transducer can designed compactly.

Nd-Fe-B permanent magnet is commonly used. Induced eddy current density of the sample and a static bias magnetic field generate the Lorentz force, the strength of the Lorentz force is proportional to the intensity of static bias magnetic field. Using the finite element software Ansys to analyses the magnetic induction, according to the principle [16] of EMAT generating Lamb wave, magnetic induction component B_S play a role on generating Lamb wave.

Changed the parameters of the permanent magnet, the distributions of the magnetic induction y-axis component perpendicular to the sample surface and eddy current distribution of the surface of the permanent magnet are studied. Fig. 3 is the EMAT 3-D solid model [12]. The paper studies the influence between the three factors of the Permanent magnet width l, thickness h, the spacing δ of the permanent magnet and coil, and the magnetic induction intensity. The ranges of the three factors are: l: 30-50 mm; t: 3-33 mm; δ: 0.1-1.0 mm. By uniform experimental design, three design variables of the Permanent magnet width l, thickness h, and the spacing δ of the permanent magnet and coil are divided into 10 equal portions, and there are 11 experiments. The maximum eddy current density J is calculated by ANSYS finite element software, are listed in Table 2.

The optimal combination of the permanent magnet parameters is: the width is 32 mm, the thickness is 30 mm, and the spacing is 1.0 mm. As can be seen from the Table 2, with the increase in the thickness of the permanent magnet, the magnetic induction increases obviously. To organize the data in the table, graph showing the magnetic induction intensity with the change of the thickness of the permanent magnet can be obtained as shown in Fig. 7.

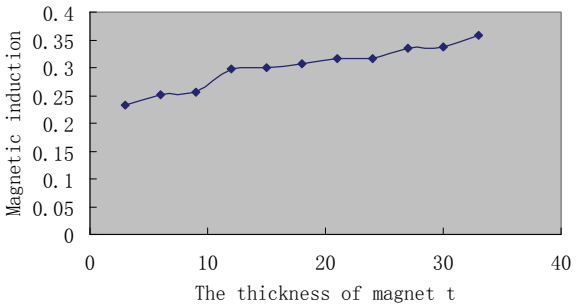

Fig. 7. The change of Magnetic induction with the influence of t.

Table 2. Uniform test of 3 elements for EMAT permanent magnet $U_{11}(11^3)$.

No.	The width of magnet a (mm)	The thickness of magnet t (mm)	Spacing δ (mm)	Magnetic induction B_S (T)
1	30	15	0.7	0.30014
2	32	30	0.3	0.33781
3	34	12	1.0	0.29875
4	36	27	0.6	0.33482
5	38	9	0.2	0.25664
6	40	24	0.9	0.31732
7	42	6	0.5	0.25083
8	44	21	0.1	0.31669
9	46	3	0.8	0.23275
10	48	18	0.4	0.30654
11	50	33	1.1	0.35786

5. Experimental Verification

Test uses the steel plate with the size of 450 mm × 450 mm × 3 mm. There is a through hole with diameter 20 mm in the center. A detection system block diagram was shown in Fig. 8.

A pulse signal generated by the signal unit outputs excites the transmitting coil after power amplification, then generates ultrasonic wave in the steel plate. Receiving coil received the electromagnetic ultrasonic signals, and after amplifying and filtering, the signal is inputted into the computer for processing through the data acquisition card.

The volume of EMAT permanent magnet is 55 mm × 55 mm × 30 mm, when the lift-off distance is 0.7 mm, Temate PowerBox H defect detection signal is shown in Fig. 9a, when the lift-off distance is 0.1 mm, Temate PowerBox H defect detection signal is shown in Fig. 9b.

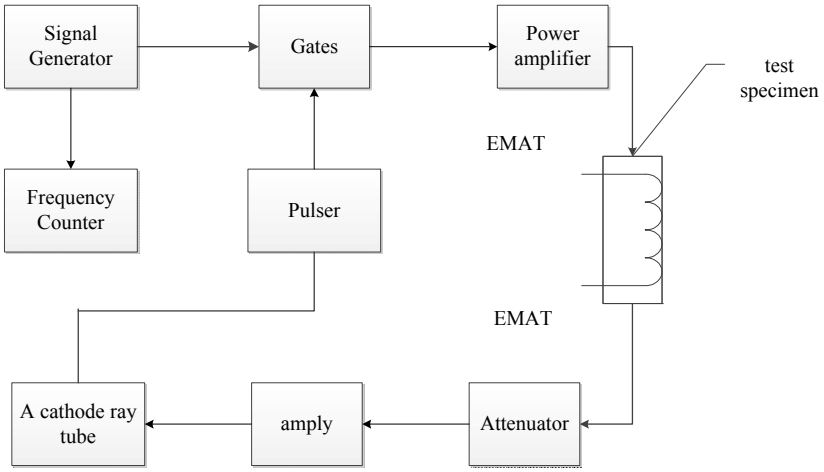

Fig. 8. EMAT detection system block diagram.

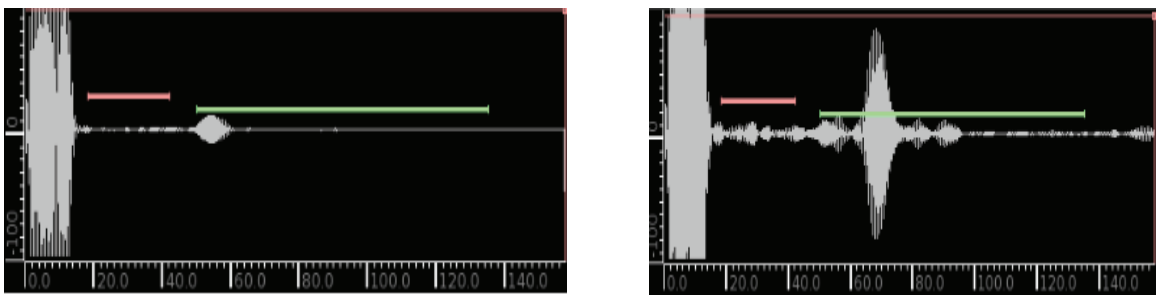

(a) the lift-off distance is 0.7 mm

(b) the lift-off distance is 0.1 mm

Fig.9 Comparison of damage signal.

6. Conclusion

An EMAT coupling model was established and used to stimulate study the influence on the detection sensitivity of the main dimensions of the EMAT coil and the EMAT permanent magnet parameters, and lift-off distance. By uniform design and finite element calculations, general law about improving EMAT detection sensitivity was obtained: under the premise that interference will not occur, the liftoff distance and the distance between the permanent magnet and the coil should be as small as possible; with the increase in the thickness of the permanent magnet, the magnetic induction increase more obviously. Weight and other factors should be taken into account when specific design.

It provides an overall principle for the optimal design of electromagnetic ultrasonic transducer.

Acknowledgements

The author thanks for the project supported by the China Postdoctoral Science Fundation (No. 20110491881) and the project supported by the Natural Science Foundation of Naval University of Engineering (HGDYDJJ13152).

References

[1]. Raymond W. Tucker, Jr., Stephen W. Kercel, Characterization of gas pipeline flaws using wavelet analysis, in *Proceedings of the 6th International Conference on Quality Control by Artificial Vision*, SPIE, Vol. 5132, 2003, pp. 485-493.

[2]. Won-Bae Na, Tribikram Kundu, Yeon-Sun Ryu, Concrete filled steel pipe inspection using electro magnetic acoustic transducer (EMAT), *Smart Structures and Materials*, SPIE, Vol. 5765, 2005, pp. 74-84.

[3]. Riichi Murayam, Kazuhiro Misumi, Development of a non-contact stress measurement system during tensile testing using the electromagnetic acoustic transducer for a lamb wave, *Independent Nondestructive Testing and Evaluation (NDT&E International)*, Vol. 39, Issue 4, 2006, pp. 299-303.

[4]. B. Dutton, S. Boonsang, R. J. Dewhurst, A new magnetic configuration for a small in-plane electromagnetic acoustic transducer applied to laser-ultrasound measurements: Modelling and validation, *Sensors and Actuators A*, Vol. 125, Issue 2, 2006, pp. 249-259.

[5]. Koorosh Mirkhani, Chris Chaggares, Chris Masterson, Optimal design of EMAT transmitters, *Independent Nondestructive Testing and Evaluation (NDT&E International)*, Vol. 37, Issue 6, 2004, pp. 181-193.

[6]. Wang Shu-Juan, Kang Lei, Li Zhi-Chao, Zhai Guo-Fu, 3-D finite element analysis and optimum design of electromagnetic acoustic transducers, in *Proceedings of the CSEE*, Vol. 29, Issue 30, 2009, pp. 123-128.

[7]. Zhu Hongxiu, Wu Miao, Liu Zhuoran, Study on optimized design of electromagnetic acoustic transducer for steel pipe default detection, *Chinese Journal of Scientific Instruments*, Vol. 27, No. 12, 2006, pp. 1734-1737.

[8]. Ni Yuan, The detection and imaging of ultrasonic Lamb wave in plate, Dissertation, *Wuhan Institute of Physics and Mathematics, Chinese Academy of Sciences*, 2008.

[9]. Zhang Zhigang, Que Peiwen, Lei Huaming, The magnetostrictive generation of Lamb wave by electromagnetic acoustic transducer and its characters, *Journal of Shang Hai Jiao Tong University*, Vol. 40, Issue 1, 2006, pp. 133-137.

[10]. X. Jian, S. Dixon, and R. Edward, Effect on ultrasonic generation of a backplate in electromagnetic acoustic transducers, *Journal of Applied Physics*, Vol. 102, Issue 2, 2007, pp. 91-96.

[11]. Wang Shujuan, Kang Lei, Zhao Zaixin, Overview of research advances in electromagnetic acoustic transducer, *Instrument Technique and Sensor*, Vol. 5, 2006, pp. 47-50.

[12]. Gao Song Wei, Zhou Jia Wei, Yang Lijian, Three-dimensional finite element analysis on radiation sound field of electromagnetic ultrasonic surface wave, *Journal of Shenyang University of Technology*, Vol. 34, Issue 2, 2012, pp. 192-197.

[13]. Ren Xiaoke, Li Jian, Simulation research on electromagnetic acoustic NDT by ANSYS, *Electronic Measurement Technology*, Vol. 31, Issue 7, 2008, pp. 26-28.

[14]. Chen Peng, Li Gu, Liu Meiquan, 3-D Finite element analysis of new EMAT roller probe, *Instrument Technique and Sensor*, Vol. 2, 2012, pp. 8-11.

[15]. Huang Lei, Design and application of EMAT transducer, *Independent Nondestructive Testing and Evaluation (NDT&E International)*, Vol. 30, Issue 1, 2006, pp. 27-28.

[16]. Huan Fengying, Zhou Zhenggan, Effect of static bias magnetic field on electromagnetic acoustic transducer sensitivity, *Journal of Mechanical Engineering*, Vol. 47, Issue 10, 2011, pp. 1-7.